27th International Congress
on Sound and Vibration
The annual congress of
the International Institute
of Acoustics and Vibration (IIAV)

11-16 July, 2021

ICSV27

Annual Congress of the International Institute of Acoustics and Vibration (IIAV)

BEAMFORMER-BASED ESTIMATION OF LONGITUDINAL WAVE SPEED IN TONEWOOD

Raffaele Malvermi, Mirco Pezzoli, Fabio Antonacci and Augusto Sarti
Departement of Electronics, Information and Bioengineering, Politecnico di Milano, Milano, Italy
e-mail: raffaele.malvermi@polimi.it

Mechanical properties of the wood have great impact on the design of musical instruments. As a matter of fact, luthiers accurately select tonewoods according to some desired elastic features. Typically, their choices are based on the longitudinal wave speed. In order to avoid direct parameter estimation techniques which can bring wood specimens to rupture, either empirical rules of thumb or expensive equipment with high sampling frequency are customarily employed. In this paper we propose a methodology for speed estimation starting from impulse responses acquired by accelerometers placed at the block edges. The technique relies on the definition of the Delay And Sum (DAS) beamformer, where instead of steering the beamformer to different Directions of Arrival (DOAs), we evaluate the filter output varying the wave speed. The proposed method is non-invasive, low-cost and it requires only basic expertise on hammer testing. We assessed the accuracy of the estimation using both simulated signals and measures on actual tonewoods. We compared the resulting performance with that of another state-of-the-art technique working at the same sampling frequency and with the same setup. Results show the effectiveness of the beamformer also in the case of low sampling frequency and high speeds.

Keywords: material properties estimation, speed measurement, beamforming, tonewood, matched field processing

1. Introduction

The analysis of the mechanical parameters of materials represents a relevant study in the field of musical acoustics and, in particular, in acoustic instrument building. As a matter of fact, the dynamic behavior, and consequently the generated sound of musical instruments [1, 2, 3, 4], is driven also by relevant mechanical parameters of the wood. For example, the Young's modulus of a wood piece can be directly estimated by means of tensile test [5, 6, 7], or indirectly from the longitudinal wave speed i.e., waves travelling along the wood grains. The latter procedure is preferred, since differently from the tensile test, the estimation of the wave speed is easily repeatable and not destructive.

In general, the problem of the estimation of the wave speed in a medium has been solved through the so-called *matched field processing* in different domains e.g., microphone array processing [8, 9, 10], underwater acoustics [11, 12, 13, 14] and seismology [15].

As regards makers, two main techniques are commonly adopted for the estimation of the longitudinal wave speed. Traditionally, luthiers estimate the longitudinal wave speed in tonewood through a procedure known as *tap tone* [16]. This technique computes the wave speed from the resonance frequency of the wood piece under the assumption that the specimen can be described as a bar. Therefore, the *tap tone* requires great skills in order to estimate the resonance frequency by *tapping* the wood piece manually.

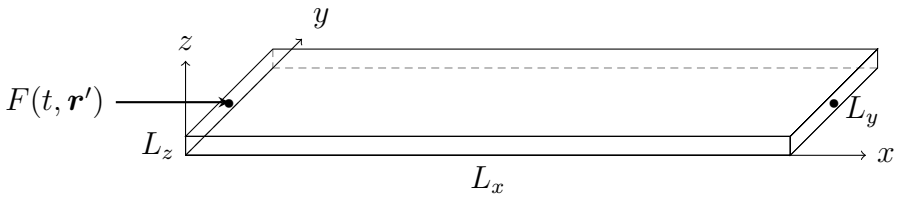

Figure 1: Geometrical representation of a tonewood plate with axial load $F(t, \boldsymbol{r'})$ and sensors placed at marked locations.

As an alternative, the Time Of Flight (TOF) estimation [17, 18] has been widely adopted among luthiers. In this case, the wave speed is computed from the measurement of the time required by an impulsive wave to travel between the endpoints of the wood piece. With the TOF estimation, no specific skills are required, at the cost of adopting expensive instrumentation. As a matter of fact, in order to correctly measure the TOF, ultrasound sampling rate is required due to the high speeds characterizing the medium. A second drawback of the TOF technique concerns its sensitivity to measurement errors since the estimation is limited to the direct wave.

Recently, in order to overcome the main limitations of the aforementioned techniques, a novel methodology for the wave speed estimation has been presented in [19]. Differently from the TOF estimate, the analysis of the signals has been extended from the direct wave to a larger portion of the impulse response. Therefore, [19] allows to work with accelerometers in the audio bandwidth. The wave speed is estimated in a practical rake receiver approach [20], where only a limited number of reflections is considered; this leaves room for improvement towards techniques employing the whole signals.

In this paper, we introduce a beamformer-based technique for the estimation of the longitudinal wave speed in tonewood. Beamforming is a well-known operation in sensor array processing [21]. It can be thought as a spatial filtering operation where the filter is designed in order to obtain a "bandpass" response for a target direction of arrival, also known as spatial frequency. Therefore, beamforming is typically employed for estimating the direction of arrival of sources or the extraction of the signal thereof [21, 22, 23]. Here, we show how the problem of estimating the longitudinal wave speed can be rephrased in terms of a beamforming operation, processing the signals acquired by a impact hammer test on the wood piece. Since the setup used in this work is akin to the one in [19], the performance of the proposed technique is assessed through a comparison with the rake receiver method. Such comparison is devised using both synthetic and measured data.

The rest of the paper is organized as follows. In Sec. 2 an interpretation of the signals observed is given. In Sec. 3 we present the proposed beamformer-based solution for the longitudinal wave speed estimation. In Sec. 4 we validate the proposed technique by means of both simulations and measurements performed on actual wood pieces. Finally, Sec. 5 draws some conclusions.

2. Problem Formulation

Let us consider a wooden plate with length L_x and constant cross-section $A = L_y \times L_z$, where L_y and L_z represent the tonewood dimensions along the y and z axes, respectively. Fig. 1 shows a visual representation of the aforementioned shape. Data are acquired with $N = 2$ accelerometers placed one at each of the two sides orthogonal to the x axis, thus located at points $\boldsymbol{r}_n = [x_n, y_n, z_n]^T$ such that $x_n = \{0, L_x\}$, $y_n = y'$, $z_n = z', \forall n = 1, \ldots, N$. To excite the system, an axial load $F(t, \boldsymbol{r'})$ is applied, where $\boldsymbol{r'} = [0, y', z']^T$. The application of loads in solids leads to the generation of elastic waves propagating through the material [24]. Three types of waves can be identified, namely *longitudinal*, *transverse* and *bending*, according to the direction in which the displacement of particles is observed.

Assuming the setup presented, only longitudinal displacement is expected to be measured by sensors. Therefore, the system vibration can be modelled by means of the one-dimensional longitudinal wave equation, i.e.

$$\frac{\partial^2 u(t,x)}{\partial t^2} = c^2 \frac{\partial^2 u(t,x)}{\partial x^2}, \tag{1}$$

where $u(t,x)$ represents the axial displacement of the specimen, either an elongation or a contraction, and c is the longitudinal wave speed.

In general, the solution to Eq. (1) can be modelled as the convolution between the source signal given by the axial load and the system response. A generalized solution in the frequency domain is

$$S(\omega, \boldsymbol{r_n}) = H(\omega, \boldsymbol{r'}, \boldsymbol{r_n})\Gamma(\omega, \boldsymbol{r'}) + B(\omega, \boldsymbol{r_n}), \tag{2}$$

where $\Gamma(\omega, \boldsymbol{r'})$ is the source signal, $H(\omega, \boldsymbol{r'}, \boldsymbol{r_n})$ is the Transfer Function (TF) of the block between $\boldsymbol{r'}$ and $\boldsymbol{r_n}$ and $B(\omega, \boldsymbol{r_n})$ represents additive white noise at the nth sensor. The TF takes into account the direct path and the reflections at the block boundaries, thus the acquired signals can be seen as the combination of attenuated and delayed replicas of $\Gamma(\omega, \boldsymbol{r'})$, whose delays depend only on speed c. The longitudinal speed c is a good estimator for assessing the elasticity of a tonewood block, since it can be expressed in terms of specific coefficients belonging to its material elasticity tensor [3]. In particular, when considering thin plates, a slight expansion along the direction orthogonal to the wavefront occurs performing a local alteration of the stiffness and leading to

$$c = \sqrt{\frac{E}{\rho(1-\nu^2)}}, \tag{3}$$

where E, ν and ρ are the Young's modulus, the Poisson's ratio and the density of the material, respectively.

3. Beamformer-based wave speed estimator

In this manuscript, we propose to model $H(\cdot)$ in Eq. (2) as the steering vector of a classical Delay And Sum (DAS) beamformer [21], assuming the aligned sensors in the setup considered as a linear uniform array. Moreover, since the direction of the plane wave is known and fixed along the longitudinal axis, the beamformer definition can be evaluated assuming the wave speed as the parameter to estimate.

Let us consider a scenario where a narrowband source with carrier frequency ω and $N > 1$ sensors with flat response are located over a 2D space. Assuming far-field and homogeneous propagation through the medium [25, 26], Eq. (2) can be rephrased in matrix form as

$$\mathbf{s}(\omega) = \mathbf{a}(c)\Gamma(\omega) + \mathbf{b}(\omega), \tag{4}$$

where $\mathbf{s} \in \mathbb{C}^{N\times 1}$ is the vector of the signals Eq. (2), $\mathbf{b} \in \mathbb{C}^{N\times 1}$ represents the noise component for the N sensors and $\mathbf{a}(c) \in \mathbb{C}^{N\times 1}$ is the propagation vector modelling the delays applied on a plane wave when approaching each sensor.

In the case of a linear array of uniformly spaced sensors with spacing d (see Fig. 2(a)), each element of the propagation vector $\mathbf{a}(c)$ can be defined as [21]

$$[\mathbf{a}(c)]_n = e^{-j\frac{\omega d \sin\theta}{c}(n-1)} = e^{-j\mathrm{F_s}(n-1)}, \quad n = 1, \ldots, N, \tag{5}$$

where $\mathrm{F_s}$ is the so-called *spatial frequency*, namely

$$\mathrm{F_s} \triangleq \frac{\omega d \sin\theta}{c}, \tag{6}$$

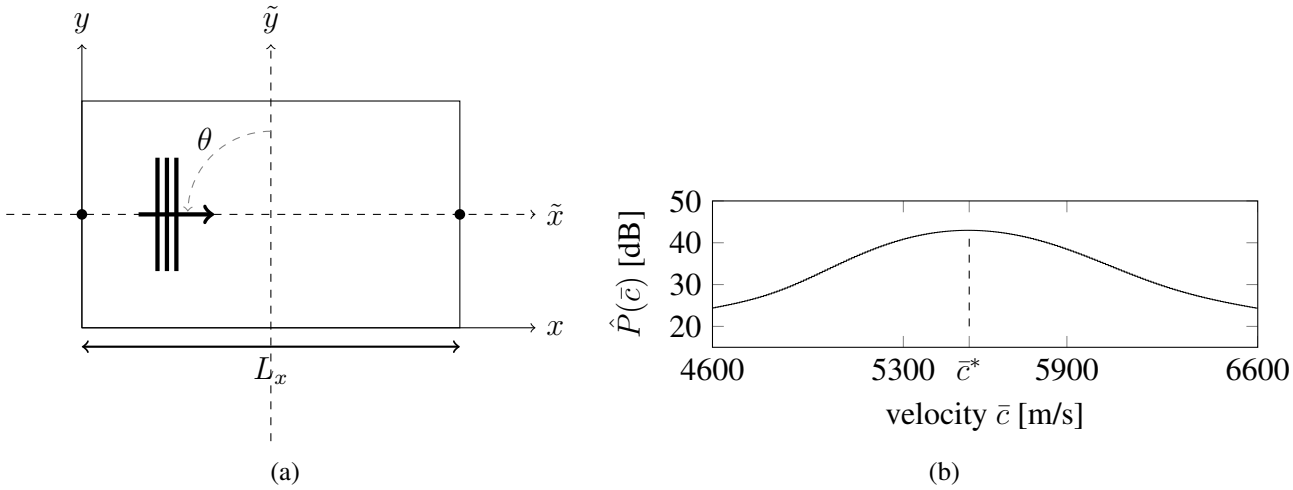

(a) (b)

Figure 2: Linear uniform sensor array according to the proposed setup (a) and example of pseudospectrum $\hat{P}(\bar{c})$ generated through simulations and averaged over multiple temporal frequencies ω (b). In the setup proposed, $N = 2$ sensors are placed one at each specimen edge, with spacing $d = L_x$. According to the array reference system with axes $\tilde{x}$ ($y = y'$) and $\tilde{y}$ ($x = L_x/2$), the plane wave has direction $\theta = \pi/2$. The desired longitudinal speed $\bar{c}^*$ can be estimated from $\hat{P}(\bar{c})$ as the location of its maximum.

with $\theta \in \{-\frac{\pi}{2}, \frac{\pi}{2}\}$ the direction of propagation of the plane wave and c the wave speed. Intuitively, we can interpret the sensor array setup as a spatial sampling of the waves in Eq. (5) that corresponds to a spatial frequency representation in Eq. (6). According to the setup proposed in Section 2 and depicted in Fig. 2(a), the geometric parameters characterizing ω_s in Eq. (6) are known and fixed ($\theta = \frac{\pi}{2}$ and $d = L_x$, respectively), thus leading to

$$\mathrm{F_s} = \frac{\omega L_x}{c}, \tag{7}$$

where $\mathrm{F_s}$ is expressed as a function of the unknown longitudinal wave speed c.

Given the signals $\mathbf{s}$ in Eq. (4), the DAS beamformer can be seen as a spatial filter whose weights $\mathbf{h}(c) \in \mathbb{C}^{N\times 1}$ are searched within the parameter space of velocity candidates in order to maximize the output signal power in correspondence of a target value $\bar{c}$. The corresponding optimization problem can be formulated as [21]

$$\arg\min_{\mathbf{h}} \qquad E\{|\mathbf{h}^H\mathbf{s}|^2\} \tag{8a}$$

$$\text{subject to} \qquad \mathbf{h}^H(\bar{c})\mathbf{a}(\bar{c}) = 1, \tag{8b}$$

where $p = \mathbf{h}^H\mathbf{s}$ is the filtered signal. Assuming that the signal is spatially white, i.e. $\mathbf{s}\mathbf{s}^T = \mathbf{I}_N$ with $\mathbf{I}_N$ the $N \times N$ identity matrix, the solution to Eq. (8a) leads to the optimal filter

$$\mathbf{h}(\bar{c}) = \frac{\mathbf{a}(\bar{c})}{N}. \tag{9}$$

Once the filter is defined, the desired longitudinal wave speed $\bar{c}^*$ can be estimated by evaluating the so-called *pseudospectrum* of the beamformer, defined as

$$P(\bar{c}) = E\{|p(\bar{c})|^2\} = \frac{\mathbf{a}^H(\bar{c})\mathbf{a}(\bar{c})}{N^2}, \quad \text{such that} \quad \bar{c}^* = \arg\max_{\bar{c}} P(\bar{c}). \tag{10}$$

In practice, we evaluate the pseudospectrum in Eq. (10) for a set of candidate velocities within a range $[c_{\min}, c_{\max}]$ defined accordingly to the material under analysis. It is worth noticing that both the

signal in Eq. (2) and the beamforming in Eq. (5) assume a narrowband source signal, thus a fixed value of the temporal frequency ω. However, the spatial frequency domain can be extended for wider frequency intervals so that the Nyquist theorem is satisfied. In particular, since the motion of the longitudinal waves implies bouncing at the plate edges, temporal frequencies ω are selected in order to consider only wavelengths compatible to the block length, such that

$$\frac{\omega}{c} = \frac{\pi}{L_x}, \quad \text{with} \quad c \in [c_{\min}, c_{\max}]. \tag{11}$$

Given the evaluation of the pseudospectrum over a set of K temporal frequencies $P(\bar{c}, \omega_k)$, an averaged indicator $\hat{P}(\bar{c})$ can thus be devised to increase the robustness of the estimate, namely

$$\hat{P}(\bar{c}) = \frac{1}{K} \sum_{k=1}^{K} P(\bar{c}, \omega_k). \tag{12}$$

Fig. 2(b) shows an example of $\hat{P}(\bar{c})$ where the maximum and the corresponding optimal speed $\bar{c}^*$ are highlighted.

4. Validation

We tested the beamformer-based speed estimation both on simulated signals and data measured from actual tonewood specimens. The first case study is analyzed with the aim to assess the accuracy of the results knowing the target values. The second experiment presents the application of the proposed method on a real case scenario to evaluate the variability of the estimates when obtained from multiple independent acquisitions. The performance of the beamformer is compared to that of the rake receiver technique [19].

A pre-processing step has been devised on input signals to improve the signal-to-noise ratio [27, 28], similarly to [19]. Simulations, pre-processing and estimation have been implemented in *MATLAB*.

4.1 Simulations

We have simulated several blocks of homogeneous isotropic material with rectangular cross-section, variable length $L_x \in [0.5, 1]\mathrm{m}$, width $L_y = 0.15\,\mathrm{m}$ and thickness $L_z = 0.03\,\mathrm{m}$. A set of aligned impulse responses have been generated for each solid using the image source method [29, 30] to include multiple reflections. The wave speed has been varied within the range $c \in [1000, 8000]\mathrm{m/s}$ with a step equal to $500\,\mathrm{m/s}$ and the signals obtained have been sampled at a sampling frequency equal to $22.05\,\mathrm{kHz}$. Gaussian white noise has been added to model a signal-to-noise ratio equal to $60\,\mathrm{dB}$. The estimation accuracy has been evaluated in terms of the relative error

$$\varepsilon_{rel}(c) = \left| \frac{c - \bar{c}^*}{c} \right|, \tag{13}$$

where c is the actual longitudinal speed used during simulations and $\bar{c}^*$ is the corresponding prediction computed in (10).

Fig. 3 shows a comparison between the values of Eq. (13) obtained in a rake receiver fashion (Fig. 3(a)) and using the beamformer (Fig. 3(b)) for all the pairs (L_x, c) considered. In general, the proposed method outperforms the competitor with $\varepsilon_{rel} \leq 0.016$ $(1.6\,\%)$ against the $5\,\%$ upper bound encountered in [19]. In particular, better estimations are provided with high velocities $(4000 - 7000\ \mathrm{m/s})$ and small lengths $(0.5 - 0.65\ \mathrm{m})$, which are reasonable values for actual tonewood blocks.

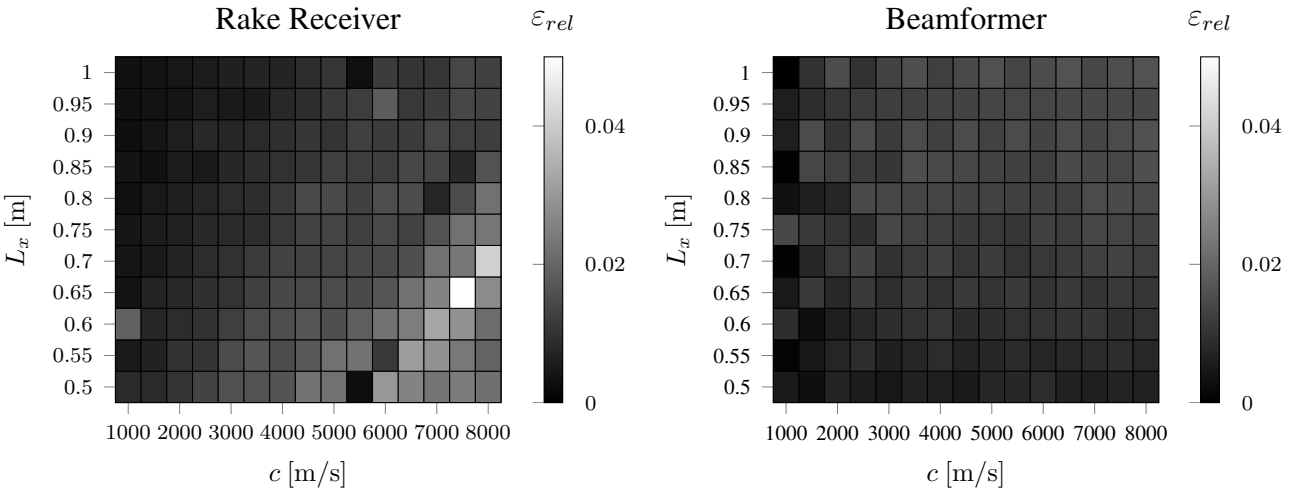

Figure 3: Relative error of the estimation with respect to expected speed in simulated data. Comparison between rake receiver-based (a) and proposed (b) techniques, varying the specimen length L_x and the groundtruth c.

Inspecting Fig. 3(b), a slight worsening in the beamformer performance can be noticed for increasing values of c. This behavior is expected, since the elements of the steering vector in Eq. (9) will tend to 1, thus lowering the beamformer resolution capability. Although this can result in poorer predictions when considering higher speed intervals, results are good in the range of interest for tonewood blocks.

4.2 Measurements

The responses of $W = 8$ rectangular spruce thin plates have been measured by means of impact hammer testing. During the measurements, each specimen was suspended using rubber bands in order to simulate free boundary conditions at its edges. Wood specimens are grouped in pairs, each belonging to the same tree and thus sharing similar elastic properties. All the specimens are characterized by the same shape, with $L_x = 0.45\,\mathrm{m}$, $L_y = 0.19\,\mathrm{m}$ and $L_z = 0.003\,\mathrm{m}$. We have acquired a total of 5 impulse responses for each wood block using a dynamometric impact hammer with light tip (086E80) and $N = 2$ uniaxial accelerometers (352A72) by *PCB Piezotronics*. Fig. 4(a) presents some of the signals acquired. Signals have been sampled with sampling frequency equal to $48\,\mathrm{kHz}$.

We have applied both the rake receiver-based technique and beamforming on single acquisitions and we have assessed the robustness of the two estimators by analyzing the mean and the standard deviation of the estimated speeds obtained for each wooden specimen.

Results are depicted in Fig. 4(b). It can be observed that all the predictions range between $5000\,\mathrm{m/s}$ and $6000\,\mathrm{m/s}$, which is in accordance with the values reported in the literature for spruce cuts selected by makers. In general, wood blocks taken from the same tree show similar estimated values for the longitudinal wave speed, except for specimens 3a and 3b where the rake receiver-based estimator shows a $400\,\mathrm{m/s}$ difference and specimens 4a and 4b where the beamformer predictions differ by an amount of $300\,\mathrm{m/s}$. It is noteworthy that the beamformer estimation is characterized by lower values of the standard deviation, reaching a maximum of $1\,\%$ in the worst case, compared to a maximum of $7\,\%$ observed for the competitor and thus proving to be a more reliable estimator.

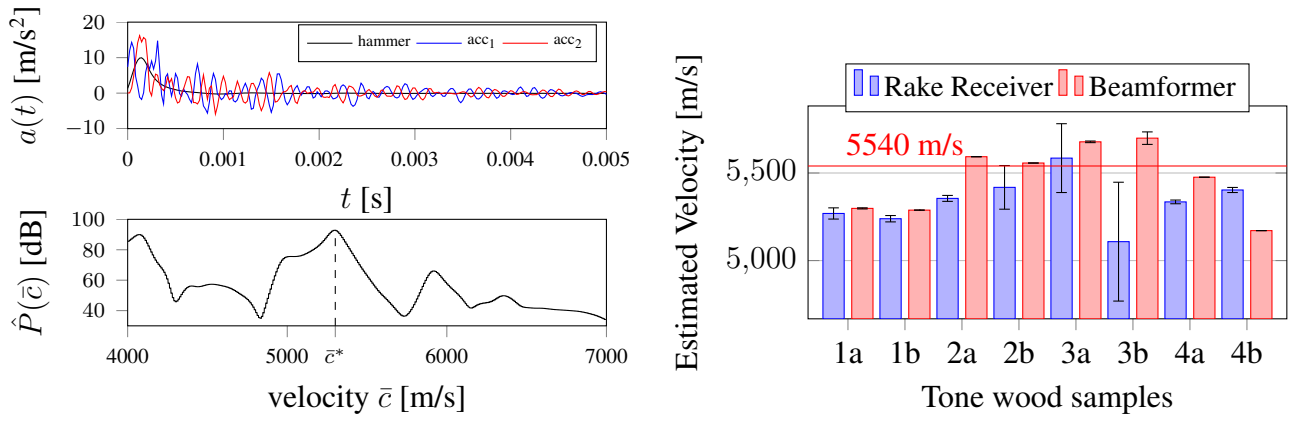

(a) (b)

Figure 4: Speed estimation on actual rectangular plates made of spruce. Plates from the same tree belong to the same pair. Examples of raw signals and the associated pseudospectrum (a) are reported along with mean and standard deviation of the estimates using the rake receiver method, in blue, and the beamformer, in red (b). A red line denotes a typical value of c estimated using Eq. (3) and spruce properties in [31].

5. Conclusions

This manuscript presents a modified version of a classical Delay And Sum Beamformer for the estimation of the longitudinal wave speed in tonewoods. The proposed method performs spatial filtering on a set of impulse responses measured by means of impact hammer testing, modelling the accelerometers aligned along the longitudinal axis of the wood block as a linear uniform sensor array.

The accuracy of the technique has been assessed using synthetic data, for which the actual longitudinal speed was known, and compared with another state-of-the-art method working with same setup and sampling frequency. The beamformer showed comparable results with respect to the competitor for low speeds while an improved estimation can be observed when considering higher values, in particular within the range of interest for tonewoods. Moreover, we tested both the techniques on a set of 8 rectangular spruce plates to evaluate the robustness of the estimators over multiple acquisitions. Both the methods gave coherent results, with the beamformer showing a better performance in terms of standard deviation. In general, the application of beamforming on the proposed data model led to promising results, which can be further improved in terms of resolution by investigating more advanced algorithms.

REFERENCES

1. Sproßmann, R., Zauer, M. and Wagenführ, A. Characterization of acoustic and mechanical properties of common tropical woods used in classical guitars, *Results in Physics*, **7**, 1737 – 1742, (2017).

2. Viala, R., Placet, V. and Cogan, S. Identification of the anisotropic elastic and damping properties of complex shape composite parts using an inverse method based on finite element model updating and 3d velocity fields measurements (femu-3dvf): Application to bio-based composite violin soundboards, *Composites Part A: Applied Science and Manufacturing*, **106**, 91 – 103, (2018).

3. Fletcher, N. H. and Rossing, T. D., *The physics of musical instruments*, Springer Science & Business Media (2012).

4. Wegst, U. G. K. Wood for sound, *American Journal of Botany*, **93** (10), 1439–1448, (2006).

5. Record, S. J., *The mechanical properties of wood: including a discussion of the factors affecting the mechanical properties, and methods of timber testing*, J. Wiley & Sons, Incorporated (1914).

6. Doyle, D. V. and Markwardt, L. J. Forest Products Lab Madison Wis, Tension parallel-to-grain properties of southern pine dimension lumber, (1967).

7. Mahajan, S., *Encyclopedia of Materials: Science and Technology*, Pergamon Press. (2001).

8. Annibale, P., Filos, J., Naylor, P. A. and Rabenstein, R. Tdoa-based speed of sound estimation for air temperature and room geometry inference, *IEEE Transactions on Audio, Speech, and Language Processing*, **21** (2), 234–246, (2013).

9. Annibale, P. and Rabenstein, R. Closed-form estimation of the speed of propagating waves from time measurements, *Multidimensional Systems and Signal Processing*, **25** (2), 361–378, (2014).

10. Rabenstein, R. and Annibale, P. Acoustic source localization under variable speed of sound conditions, *Wireless Communications and Mobile Computing*, (2017).

11. Baggeroer, A. B. and Kuperman, W. A., (1993), *Matched Field Processing in Ocean Acoustics*, pp. 79–114. Springer Netherlands.

12. Isik, M. T. and Akan, O. B. A three dimensional localization algorithm for underwater acoustic sensor networks, *IEEE Transactions on Wireless Communications*, **8** (9), 4457–4463, (2009).

13. Shiba, H. Layered model sound speed profile estimation, *MTS/IEEE OCEANS - Bergen*, pp. 1–7, IEEE Oceanic Engineering Society, (2013).

14. Skarsoulis, E. K. and Piperakis, G. S. Use of acoustic navigation signals for simultaneous localization and sound-speed estimation, *The Journal of the Acoustical Society of America*, **125** (3), 1384–1393, (2009).

15. Anderson, M. E. and Trahey, G. E. The direct estimation of sound speed using pulse–echo ultrasound, *The Journal of the Acoustical Society of America*, **104** (5), 3099–3106, (1998).

16. Jansson, E., *Acoustic for violin and guitar makers - Chapter V: Vibration properties of the wood and tuning of violin plates*, KTH Royal Institute of Technology (2002).

17. Kleinschmidt, P. and Magori, V. Ultrasonic remote sensors for noncontact object detection, *Siemens Forschungs und Entwicklungsberichte*, **10**, 110–118, (1981).

18. Marioli, D., Narduzzi, C., Offelli, C., Petri, D., Sardini, E. and Taroni, A. Digital time-of-flight measurement for ultrasonic sensors, *Transactions on Instrumentation and Measurement*, **41** (1), 93–97, (1992).

19. Villa, L., Pezzoli, M., Antonacci, F. and Sarti, A. A methodology for the estimation of propagation speed of longitudinal waves in tone wood, *2020 28th European Signal Processing Conference (EUSIPCO)*, pp. 66–70, (2021).

20. Price, R. and Green, P. E. A communication technique for multipath channels, *Proceedings of the IRE*, **46** (3), 555–570, (1958).

21. Van Trees, H. L., *Optimum array processing*, vol. 1, Wiley Online Library (2002).

22. Berkun, R., Cohen, I. and Benesty, J. Combined beamformers for robust broadband regularized superdirective beamforming, *IEEE/ACM Transactions on Audio, Speech and Language Processing*, **23** (5), 877–886, (2015).

23. Bitzer, J. and Simmer, K. U., (2001), Superdirective microphone arrays. *Microphone arrays*, pp. 19–38, Springer.

24. Norton, M. P. and Karczub, D. G., *Fundamentals of Noise and Vibration Analysis for Engineers*, Cambridge University Press, 2 edn. (2003).

25. Trees, H. L. V., *Optimum Array Processing: Part IV of Detection, Estimation, and Modulation Theory*, Wiley (2002).

26. Abhayapala, T. D., Kennedy, R. A. and Williamson, R. C. Nearfield broadband array design using a radially invariant modal expansion, *The Journal of the Acoustical Society of America*, **107** (1), 392–403, (2000).

27. Richardson, M. H. Structural dynamics measurements, *SD2000*, pp. 1–13, (1999).

28. Fladung, W. Windows used for impact testing, *Proceedings-SPIE The International Society for Optical Engineering*, pp. 1662–1666, (1997).

29. Gunda, R., Vijayakar, S. and Singh, R. Method of images for the harmonic response of beams and rectangular plates, *Journal of Sound and Vibration*, **185** (5), 791 – 808, (1995).

30. Habets, E. A. Room impulse response generator, *Technische Universiteit Eindhoven, Tech. Rep*, **2** (2.4), 1, (2006).

31. Ross, R. J., et al. Wood handbook: wood as an engineering material, *USDA Forest Service, Forest Products Laboratory, General Technical Report FPL-GTR-190, 2010: 509 p. 1 v.*, **190**, (2010).